



# Self-Assembly and Cascade Catalysis by a Soft-Oxometalate (SOM) System

Kousik Das<sup>1</sup>, Tingting Yan<sup>2</sup>, Shounik Paul<sup>1</sup>, Shilun Qiu<sup>2</sup>, Teng Ben<sup>2\*</sup> and Soumyajit Roy<sup>1\*</sup>

<sup>1</sup> Eco-Friendly Applied Materials Laboratory, Department of Chemical Sciences, Indian Institute of Science Education and Research, Kolkata, India, <sup>2</sup> Department of Chemistry, Jilin University, Changchun, China

## OPEN ACCESS

### Edited by:

Hadi Nur,  
University of Technology  
Malaysia, Malaysia

### Reviewed by:

Haralampos N. Miras,  
University of Glasgow,  
United Kingdom  
Lin Zhong,  
Sichuan University, China

### \*Correspondence:

Teng Ben  
tben@jlu.edu.cn  
Soumyajit Roy  
s.roy@iiserkol.ac.in

### Specialty section:

This article was submitted to  
Catalysis and Photocatalysis,  
a section of the journal  
Frontiers in Chemistry

**Received:** 01 September 2020

**Accepted:** 28 October 2020

**Published:** 27 November 2020

### Citation:

Das K, Yan T, Paul S, Qiu S, Ben T  
and Roy S (2020) Self-Assembly and  
Cascade Catalysis by a  
Soft-Oxometalate (SOM) System.  
Front. Chem. 8:601814.  
doi: 10.3389/fchem.2020.601814

Cascade catalysis has gained importance due to its various applications. In this work, cascade catalysis was performed using a self-assembled soft-oxometalate (SOM) as a model system. At first, we synthesized an oxometalate (OM) hybrid with a polymerizable organic cation, namely tetrakis(4-aminophenyl)methane, and an OM,  $K_8[SiW_{11}O_{39}]$ . The hybrid in turn was converted into SOM in water, DMSO mixture, and characterized by different techniques, ranging from electron microscopy to DLS. The SOM state is endowed with the ability to polymerize the aniline based counter ions associated with it in the presence of UV-light. This polymerization is possible due to the presence of photocatalytic OMs (oxometalates) in the SOMs. The polymer-SOM hybrid in cascade oxidizes selectively aniline to nitrobenzene and nitrite to nitrate owing to the residual oxidizing property of the OM constituents in it. This is the first example of cascade catalysis in SOM chemistry.

**Keywords:** polyoxometalate, self-assembly, polymerization, cascade catalysis, oxidation

## INTRODUCTION

Assembly of multicomponent, multifunctional architecture is a challenge. For instance successful assembly of organic-inorganic hybrid material (Hagman et al., 1999) leads to the emergence of non-linear unusual properties (Kagan et al., 1999; Yin et al., 2012, 2014; Dualeh et al., 2014). The achievement of a successful working design is thus an immediate challenge for chemists. As part of this process, questions emerge, as to whether it is possible to synthesize an inorganic-organic hybrid architecture based on oxometalate. Can such an assembled supramolecular architecture be functional? Here we address these questions, asking more specifically whether is it possible to design an organic moiety and oxometalate (OM) based self-assembly of a soft-oxometalate (SOM). Can such SOM be catalytically polymerized to form a SOM hybrid? Can the resulting SOM hybrid in turn show cascade catalysis? Before we answer these questions we explore the literature and explain our design.

Polyoxometalates (POMs), (Pope et al., 2004) crystalline state of transition metal oxo-clusters (oxometalates) have gained immense research interest due to their tuneable size and morphology, unique electronic properties, and wide range of applications like catalysis, electronics, nano materials, medicine etc. (Wang et al., 2003; Cronin and Müller, 2012; Lv et al., 2012; Wang and Weinstock, 2012). Due to the high oxidation states and photoexcitation properties of transition

metals, polyoxometalates are very efficient and promising catalysts (Kikukawa et al., 2012; Suzuki et al., 2015; Wang and Yang, 2015). They have been used as catalysts for water splitting (Rausch et al., 2014), polymerization (Chen et al., 2013), and several other organic reactions over the past few decades. Our group has also published a series of catalytic reactions with oxometalates in recent years (Thomas et al., 2015; Das et al., 2016a,b,c). Oxometalates have a very unique solution behavior. Depending on their counter ions and volume fraction/concentration (Thomas et al., 2018), pH (Paul et al., 2018) oxometalates can show a heterogeneous/colloidal or soft-matter state, which has been called the soft-oxometalate (SOM) state (Roy, 2011, 2014). Owing to the intrinsic OM constituents in SOMs the latter holds promise to manifest the properties of OMs in higher length scales and bulk. SOMs thus provide a platform to manifest synergistic properties by the judicious assembly of large OMs (like  $\text{PW}_{12}$  Keggin,  $\text{Mo}_{132}$ , (Verhoeff et al., 2007)  $\text{Mo}_{154}$  (Liu et al., 2003), and their counter-ions. To date, self-assembled SOMs have used simple counter-ions like protons, ammonium and alkaline earth metal ions. Such ions leave the chemistry of SOMs dormant. Hence the challenge in SOM-engineering necessitates the judicious choice of OM and counter-ions that can open up the possibilities of new SOM chemistry. If the counter-ions are reactive, redox polymerizable organic ligands like amino-phenyl methane with multiple sites, can open up a host of possibilities for self-assembly. This approach of combining molecular oxometalates with suitable organic moieties to make crystalline POM-organic hybrids has already been explored in the context of crystalline POM chemistry (Zhang et al., 2010; Chen et al., 2013). In this study we adapt this approach to SOM chemistry and demonstrate cascade catalysis for the first time.

As mentioned earlier, the choice of the OM and the organic counter ion in SOMs needs to be judicious. For instance, these units have to be mutually compatible to form SOMs and if the organic counter-ion is polymerizable then the resulting organic polymers can have direct applications (Heeger, 1993; Macdiarmid, 2001). In this regard, it is important to mention some synthetically important networks such as metal organic frameworks (MOF), (Long and Yaghi, 2009), covalent organic frameworks (COF) (Wan et al., 2009), and porous aromatic frameworks (PAF) (Ben et al., 2009; Ren et al., 2010; Xu et al., 2015), etc., which have a well-defined structure and high surface area. The high surface area of such frameworks leads to better catalyst loading and their rigid structure makes them excellent support for heterogeneous catalysis (Dong et al., 2016). Recently, conductive polymers attracted a great deal of interest because of their high electrical conductivity (Shumaila et al., 2011). Among the family of conducting polymers, polyaniline is one of the most exciting polymers, due to its unique electrical conductivity, high environmental stability, and easy synthesis.

For the past few decades, scientists have been synthetically modifying their structure to use them in more commercial applications. There are several techniques of polymerization of such aniline based monomers of which redox polymerization (Kohut-Svelko et al., 2009) is worth mentioning in the present context, as it can utilize a redox-active OM center that can be built in the SOM. This redox polymerization is facile,

attractive, and has a short induction period attracting mild conditions that are conducive to SOM chemistry (Zengin et al., 2002; Fehse et al., 2007).

As mentioned earlier, various methods for the syntheses of oxometalate-organic hybrids have been reported in the literature (Bar-Nahum et al., 2003; Dolbecq et al., 2010). However simple organic ligands have been used in most of these methods and there are very few reports on the reactivity of their side chains (Rieger et al., 2012; Lachkar et al., 2016). There are still questions as to whether it is possible to synthesize an OM-organic hybrid that can catalyze a reaction on its side chain *in-situ*. After assembling the molecular hybrid, is it possible to superstructure the architecture as a SOM? Can the resulting SOM state have catalytic properties? This study addressed these questions by synthesizing a crystalline polyoxometalate-organic hybrid from a photo-redox active lacunary Keggin  $\text{K}_8[\text{SiW}_{11}\text{O}_{39}]$  and tetrakis(4-aminophenyl)methane (Uribe-Romo et al., 2009; Liu et al., 2014) with a redox polymerizable aniline side chain which can grow to form a three dimensional polymeric network, and stabilize itself as a SOM and SOM-polymer hybrid. The SOM-polymer hybrid in turn, in the fashion of cascade catalysis, electrochemically oxidizes nitrite to nitrate and aniline to nitrobenzene. Thus, the assembly and cascade catalysis reported in this work has the following steps. First, the assembly of OMs with aniline based counter ions to SOMs; second, the catalytic formation of SOM-polymer hybrid; and third, a cascade catalytic conversion of aniline to nitrobenzene and nitrite to nitrate (Figure 1).

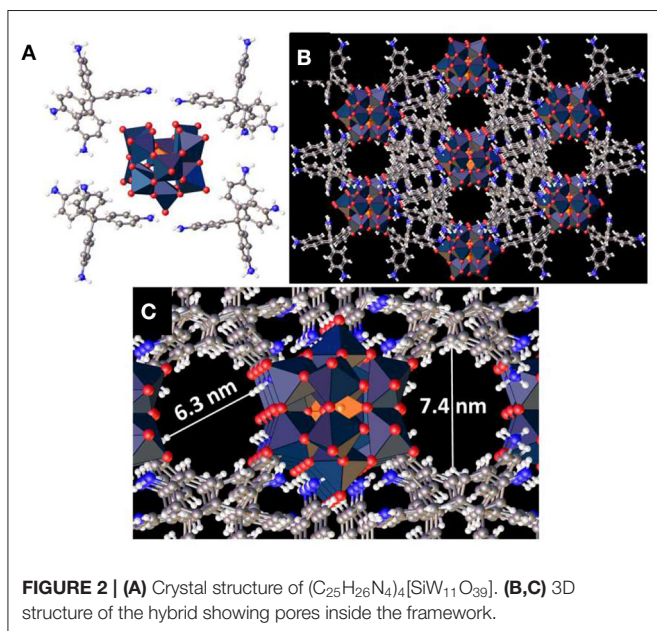
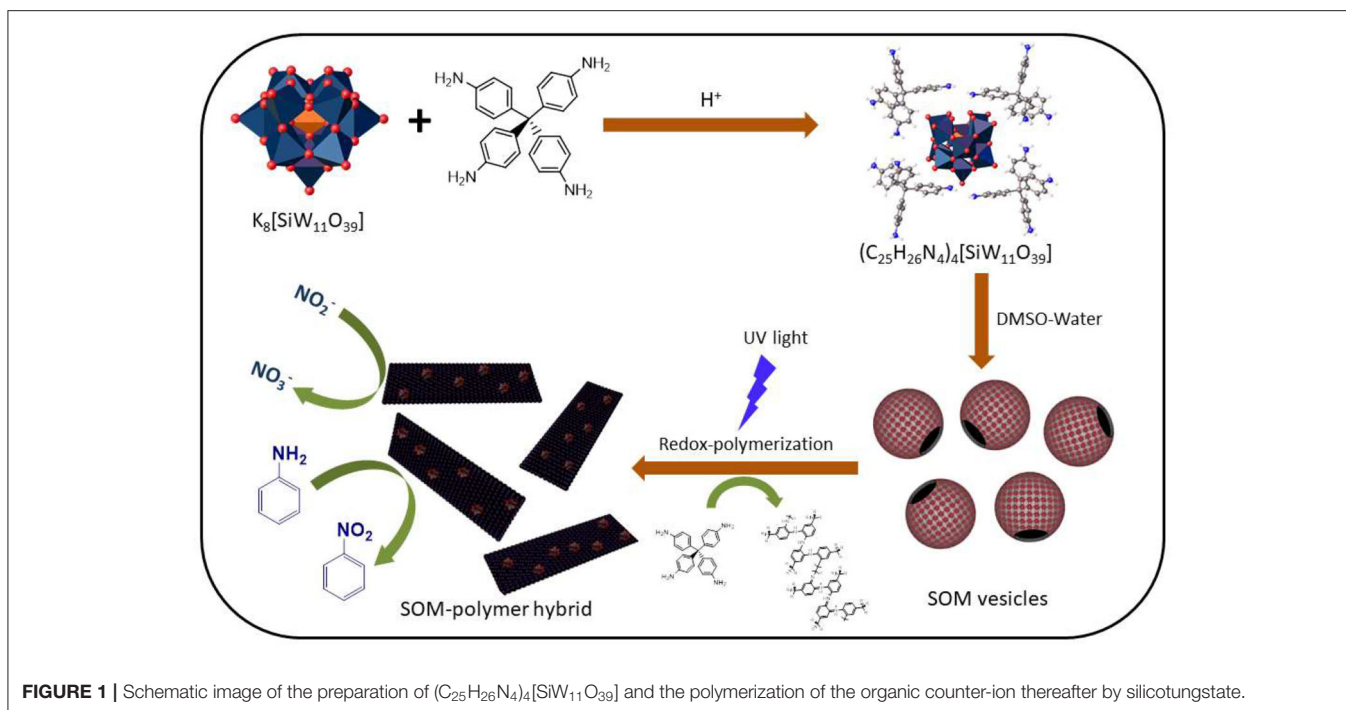
## RESULTS AND DISCUSSION

This study initially focused on the synthetic aspects of the SOM, using the following steps to investigate the reaction. First, the crystalline molecular POM-organic hybrid is synthesized and self-assembled to SOMs. Then the hybrid is polymerized. Using this polymerized hybrid, cascade catalysis was then performed.

### Synthesis and Characterization of OM-Organic Hybrid

The synthesized crystalline polyoxometalate hybrid has two components: tetrakis(4-aminophenyl)methane and  $[\text{SiW}_{11}\text{O}_{39}]^{8-}$ . To gain molecular structural insights on this hybrid we crystallized the hybrid (Figure 2A). The structure of the model compound shows that each of the oxometalate units is connected to 8 ammonium ions. It is also evident from the structure that in each organic moiety only two of the four  $-\text{NH}_2$  groups are protonated. The crystal structure also shows two different cavities with a diameter of 6.3 and 7.4 nm (Figures 2B,C). This is due to the presence of asymmetric oxometalate units in  $[\text{SiW}_{11}\text{O}_{39}]^{8-}$ . These cavities are very important for the stabilization of organic oligomers and the oxometalates present around these cavities facilitate the polymerization reaction that leads to the formation of these oligomers.

This molecular oxometalate-organic hybrid further manifests in a dispersion soft-oxometalate structural state as vesicles.



the characteristic peaks of tetrakis(4-aminophenyl)methane were found at  $1,508, 1,427\text{ cm}^{-1}$  (**Figure 3C**).

### Preparation of Soft-Oxometalate From the Hybrid

We observed that the molecular hybrid shows an amphiphilic character. It can be easily dissolved in DMSO to make a stable dispersion. A relatively low scattering intensity in the dispersion confirms the absence of any large assemblies and the hybrid remains as a discrete molecular species in solution. Upon the addition of water into the DMSO solution, the solution becomes turbid, which suggests the formation of vesicle like SOM structures in the dispersion. We have characterized the vesicles by DLS and SEM analysis. The hydrodynamic radius ( $R_h$ ) was measured by DLS (**Supplementary Figure 3**). At 1:9 DMSO water ratio, the vesicle size appears to be ca. 160 nm. In the hybrid structure, the  $[SiW_{11}O_{39}]^{8-}$  unit acts as the hydrophilic part and the organic counter ion tetrakis(4-aminophenyl)methane acts as the hydrophobic part. Since the water content is more in dispersion, we believe that in the structure the oxometalate remains on the outer surface whereas the organic part remains on the inner surface.

The size of SOM vesicles was then varied by changing the solvent polarity (Verhoeff et al., 2007). The polarity of the solvent was varied by mixing different amounts of water and DMSO. We found that the vesicle size displayed a linear relationship with the inverse of the dielectric constant of the solvent (**Figure 3B**). This implies that the vesicle size can be varied by controlling the dielectric constant of the medium, implying counter ion condensation stabilizing the dispersion.

We assume that the hybrid retains its solid-state molecular architecture in the dispersion (soft-matter state) that facilitates the polymerization reaction in the cavity (Chen et al., 2013). To further analyze the structural integrity of oxometalate as well as the organic ion, we studied the FTIR spectrum of the hybrid. The following characteristic peaks of  $[SiW_{11}O_{39}]^{8-}$ , 952, 895, 844, and  $800\text{ cm}^{-1}$  were found in hybrid oxometalate whereas

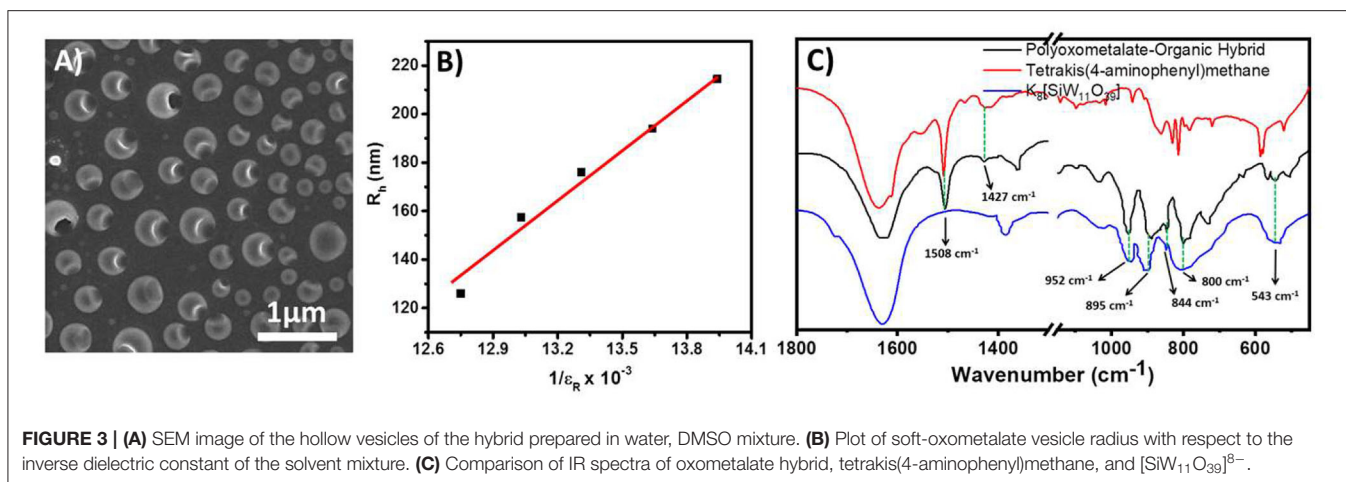


**FIGURE 3 | (A)** SEM image of the hollow vesicles of the hybrid prepared in water, DMSO mixture. **(B)** Plot of soft-oxometalate vesicle radius with respect to the inverse dielectric constant of the solvent mixture. **(C)** Comparison of IR spectra of oxometalate hybrid, tetrakis(4-aminophenyl)methane, and  $[\text{SiW}_{11}\text{O}_{39}]^{8-}$ .

The spherical nature of the vesicle was characterized by SEM analysis. The sizes obtained from SEM images are also consistent with the LS analysis (Du and Chen, 2004; Verma et al., 2005; Leng et al., 2010). Each of the vesicles shows large pores on the surface (Figure 3A) at pH 4. We believe that this is due to disruption of the surface during the drying process. However, upon adding a base, the pore(s) on the vesicle surface did not appear (Figure 4) (Sandre et al., 1999). The  $\text{pK}_b$  of aniline moiety was 9.4. At low pH (4.6) the amine group remained at an equilibrium between  $-\text{NH}_2$  and  $-\text{NH}_3^+$ . Hence the surface of the vesicle was much more labile. With the addition of a base, the pH of the solution increases, and thus the amine groups mainly remained in  $-\text{NH}_2$  form and it was less prone to disrupt the hard skin of the surface during the drying process (Liu et al., 2005; Jeong et al., 2007).

From the TEM we observed that a SOM hybrid was formed with tetrakis(4-aminophenyl)methane and  $[\text{SiW}_{11}\text{O}_{39}]^{8-}$  (Figure 5). The topology is spherical with a uniform molecular level distribution of elemental Si, W, O, N in the mesoscopic SOM structure (Figure 6B). We believe that the positively charged ammonium ions behave as an anchor for attaching the negatively charged oxometalates via electrostatic interaction.

### In-situ Polymerization of the Hybrid

We then explored whether the hybrid possessed any catalytic properties. Oxometalates are well-known for their photocatalytic properties. Recently, we photo-polymerized monomers like styrene, and acrylic acid, etc., with  $\text{PW}_{12}$  based polyoxometalate in the presence of UV radiation. This approach polymerizes the monomers via cation-radical polymerization. In the present case, the  $[\text{SiW}_{11}\text{O}_{39}]^{8-}$  also catalyzes the polymerization reaction of the tetrakis(4-aminophenyl)methane monomer in presence of UV-light (Supplementary Figure 4). The structure of the hybrid also plays an important role in polymerization. The solid state structure of the hybrid has cavities in it. We believe the hybrid retains its solid state structure in the dispersion (soft-matter state) through the formation of soft-oxometalate. We have previously shown that these cavities stabilize the monomer and facilitate the formation of the polymer (Chen et al., 2013). In this case, also, we believe that the monomers are stabilized in the structural cavity and the oxometalates present in the cavities polymerize

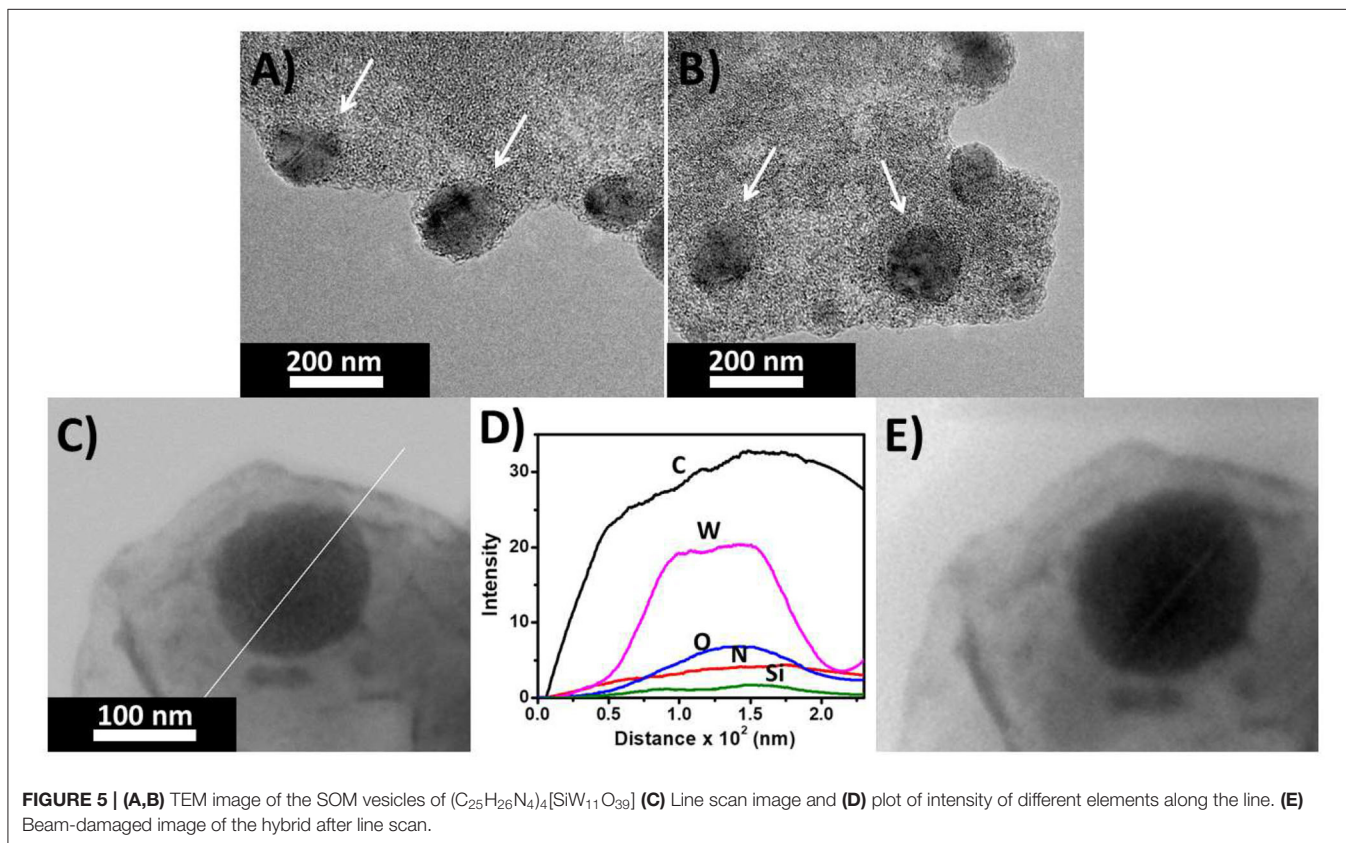
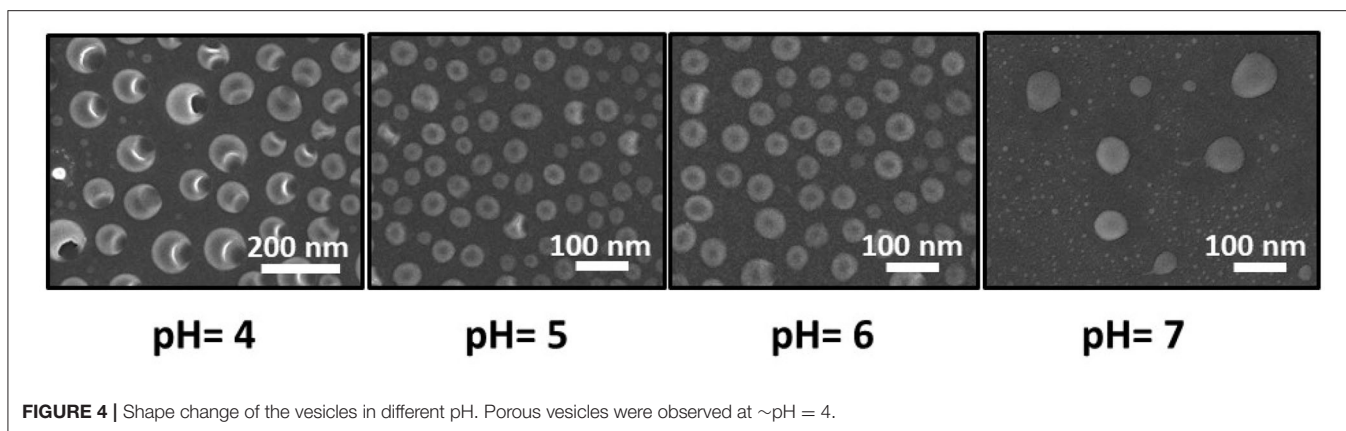
the monomers via photoredox polymerization. Tetrakis(4-aminophenyl)methane has four aniline units in its structure and can be polymerized by an oxidation reaction. The polymerization of the monomer happens in 2 weeks without any catalyst but in presence of oxometalate, the polymerization reaction happens in just 8 h (Supplementary Figure 8).

### Characterization of the Polymer

The FTIR study showed several new peaks (985, 1,215, 1,322, and  $2,576\text{ cm}^{-1}$ ) after polymerization. The peaks ranging from  $1,570$  to  $1,600\text{ cm}^{-1}$  occur because of the  $\text{C}=\text{N}$  stretching of the quinoid structure (Figure 6A) (Mostafaei and Zolriasatein, 2012).

$^1\text{H}$  and  $^{13}\text{C}$  NMR analysis of the polymer also showed several changes in the spectra, which confirms the polymerization of the monomer (Supplementary Figures 10–16). The peaks ranging from 6 to 8 ppm in the  $^1\text{H}$  spectrum are due to the aromatic protons present in the polymeric structure (Supplementary Figure 11) (Yasuda and Shimidzu, 1993). The peaks at 148 and 150 ppm in  $^{13}\text{C}$  NMR also confirm the presence of the quinoid structure of the polymer (Supplementary Figure 16). The  $\text{H}^+$  ions present in the solution attach with the nitrogen atoms of the polymer to form ammonium or iminium ions. We believe that this is because the polymer is still charged (ammonium or iminium ion) and the oxometalate remains electrostatically attached to the polymer. This is also evident from the FTIR spectrum of the polymer, which shows both the peaks of the polymer as well as the silicotungstate ion in the resultant polymer hybrid (Figure 6A).

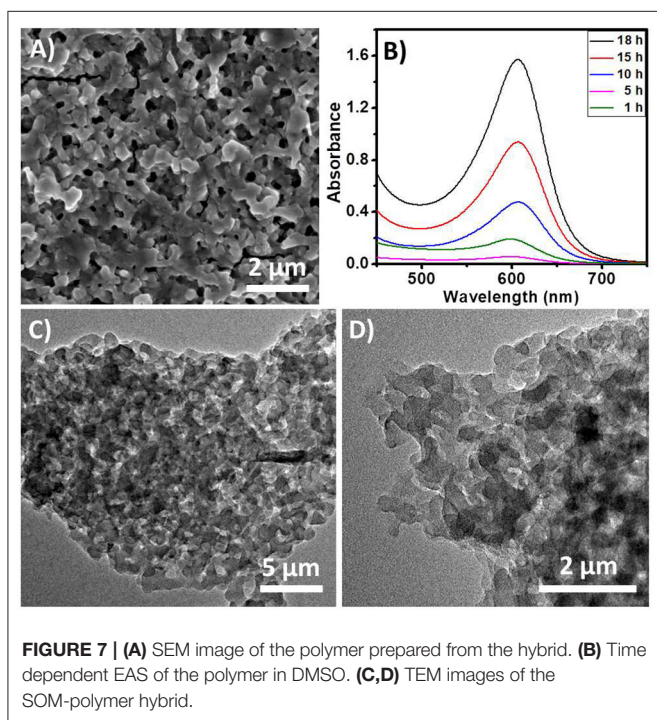
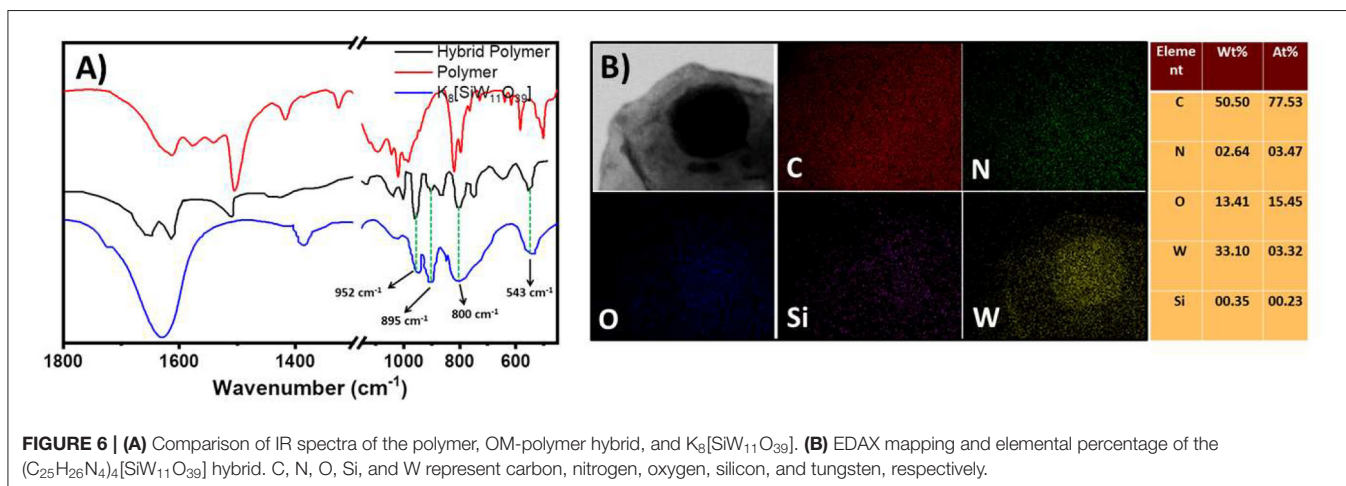
The EAS of the polymer shows a peak at 600 nm (Figure 7B). This peak corresponds to the blue color of the solution. These observations also suggest that the polymer has an emeraldine structure. The absorption band at 600 nm corresponds to the  $n-\pi^*$  transitions of the quinine-imine groups (Yasuda and Shimidzu, 1993; Sapurina and Stejskal, 2008; Liu et al., 2010; Sapurina and Shishov, 2012). The band intensity increases with time, which suggests the formation of more polymeric structures. SOM-polymer hybrid has also been characterized by SEM and TEM (Figure 7). From the EDAX mapping of the hybrid (Figure 8B), we observed that the OMs are homogeneously



distributed on the polymer surface. To locate the oxometalates in this hybrid polymer, we used porosity measurements. The BET surface areas of the chemically synthesized polymer and that of the SOM-Polymer hybrid are 19 and 14  $m^2/g$ , respectively (Figure 8A). We believe that some of the pores present in the polymer are filled by the oxometalates and hence the measured surface area is less in the polymer-oxometalate hybrid.

This study then addressed whether it is possible to change the chain length of the polymer. The chain length variation was achieved by changing the loading of oxometalate in the dispersion. The same amount of monomer was dissolved in five reaction vessels and then a different amount of OM was added to it. The reaction vessels were kept for 1 day to polymerize. The polymers were then separated from the solution

and their chain length and molecular weight were measured by viscometry (Supplementary Table 2). The empirical rule of Mark-Houwink relation was used to measure the molecular weight of the polymers (Rana et al., 2011). We observed that the molecular weight, as well as the chain length of the polymer, decreases with the increased loading of oxometalate in the starting SOM (Table 1). The plot of the molecular weight of the polymer and loading of oxometalates shows a linear decrease (Supplementary Figure 9). This indicates that the polymerization happens via radical pathway. To ensure the operation of the radical pathway in the reaction, we added catechol to the reaction mixture as a radical quencher and the polymerization reaction did not take place in the presence of catechol.



The chain length variation of the polymer is also evident from the different colors of the polymers dissolved in DMSO (**Supplementary Figure 7B**). This was because, as the chain length varies, the number of monomer units vary, and hence the degree of conjugation also varies. The different extent of conjugation in the different polymers leads to different colors of the solution. In electronic absorption spectra (EAS), the intensity of the 578 nm peak also decreases with the increase in polymer chain length (**Supplementary Figure 7A**). This is due to the presence of fewer polymer units in higher chain length polymers. The peak at 460 nm in EAS suggests the formation of the emeraldine of the polymer. We think that with the increase in OM concentration, the acidity of the solution increases, and hence more imine nitrogen gets protonated to give emeraldine salt of the polymer.

## Oxidation of Aniline to Nitrobenzene

The selective oxidation of aniline to nitrobenzene is very important in industrial synthesis. The oxidation of aniline leads to several products namely nitrosobenzene, nitrobenzene, azoxybenzene, azobenzene, etc. (Zhu and Espenson, 1995; Priewisch and Rück-Braun, 2005; Tundo et al., 2008; Shiraiishi et al., 2014). Although there are various reports in the literature involving aniline oxidation, very few have reported selective oxidation toward nitrobenzene (Meenakshi et al., 2018). Even some polyoxometalates as well as polyoxometalate-organic hybrids have been employed for the oxidation of aniline, although they require harsh reaction conditions and the catalyst has low selectivity and low recovery.

In this article, we have utilized the polymer-SOM hybrid as a catalyst for the oxidation of aniline (**Figure 9**). Due to the presence of redox active W centers and a robust support structure of the polymer network, the polymer-SOM hybrid acts as an excellent catalyst. The reaction was performed in the presence of  $H_2O_2$  at  $50^\circ C$ . In this reaction condition, the polymer-SOM hybrid oxidizes aniline selectively to nitrobenzene. A negligible amount of nitrosobenzene was also detected. All the products were detected in gas chromatography (**Supplementary Figure 5**). To check the role of solvent, the reaction was carried out in different solvents (**Supplementary Table 1**). The catalyst was recovered after each catalytic cycle (**Supplementary Figure 6**). The highest yield was detected in acetonitrile and lowest in  $H_2O$ . It should also be noted that a very good yield was also detected in DMSO. However the recovery of the catalyst is low compared to other solvents. An increase in reaction temperature, increases the reaction rate, although a small amount of azoxybenzene was also detected at a higher temperature. At lower temperatures, the reaction rate was comparatively slow. Hence the optimum temperature was set to  $50^\circ C$ . In contrast, the polyoxometalate ( $K_8[SiW_{11}O_{39}]$ ) has less conversion efficiency, and selectivity is also very low in the same reaction condition. It is also worth mentioning that the ( $K_8[SiW_{11}O_{39}]$ ) is very unstable and thus has low recovery (**Table 2**).

By definition, a cascade reaction comprises two steps where the second reaction happens because the chemical change occurs in the first step. In our case, the first step is the polymerization

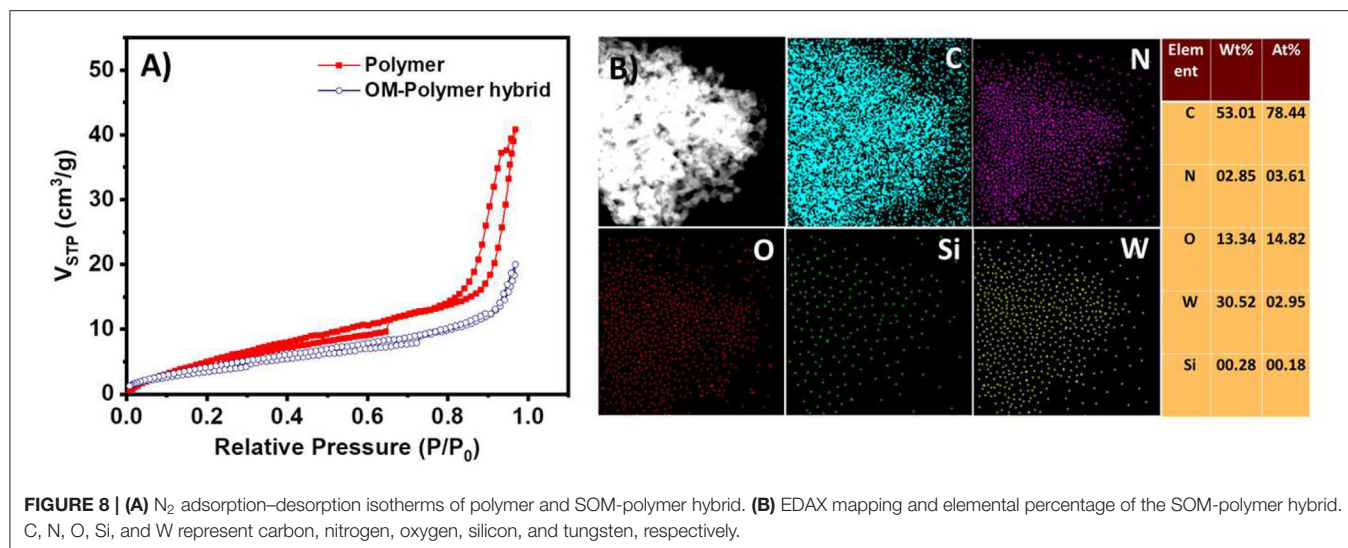


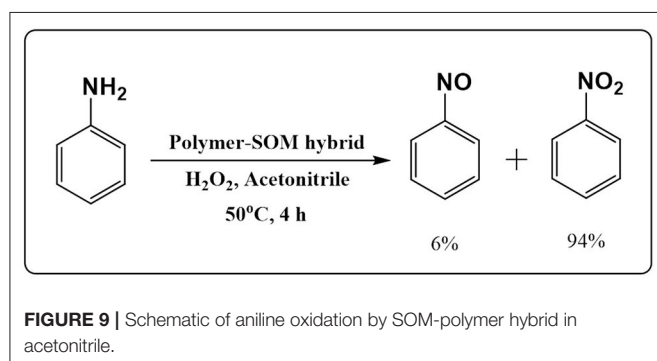
**TABLE 1 |** Chain length variation of the polymer by changing the amount of catalyst.

Sample no.	Amount of OM (mmol)	Amount of monomer (mg)	Molecular weight (kDa)
1	0.4	1	14
2	0.6	1	9.5
3	0.7	1	8.2
4	0.9	1	6.9
5	1.0	1	1.5

**TABLE 2 |** Comparison of aniline oxidation<sup>a</sup> to nitrobenzene by different catalysts.

Catalyst	Total conversion (%)	Products (%)		Recovery
		Nitrosobenzene	Nitrobenzene	
SOM-polymer	96	6	94	91
$K_8[SiW_{11}O_{39}]$	71	78	22	48

<sup>a</sup>Aniline (1 mmol), 30%  $H_2O_2$  (3 mmol), acetonitrile (5 mL), catalyst (5 mg), 50°C, stirred for 4 h.



of tetrakis(4-aminophenyl)methane by  $[SiW_{11}O_{39}]^{8-}$  in the presence of UV light. The SOM in-turn transforms into an SOM-polymer hybrid. The second step is the catalysis reaction performed by the SOM-polymer hybrid. The SOM-polymer can oxidize nitrite to nitrate electrochemically or selectively oxidize aniline to nitrobenzene thermally. In both cases, the catalysis does not occur with the SOM or the monomer and oxometalate alone. This is where cascade catalytic property emerges due to the presence of various interactions in the SOM-polymer hybrid. The polymeric network forms during the first photocatalytic experiment and endows the SOM-polymer with an emergent catalytic activity that manifests during the aniline

oxidation and carries out the concluding steps of cascade catalysis during nitrite oxidation. Without the polymeric network, the OM ( $[SiW_{11}O_{39}]^{8-}$ ) has less stability, low conversion, and poor selectivity toward aniline oxidation.

To check the stability of the catalyst we have performed IR and EAS spectroscopy. After the reaction of aniline oxidation, the recovered catalyst was thoroughly washed with ethanol and water and dried over vacuo. For IR spectroscopy the powdered catalyst was used, whereas the catalyst was dissolved in DMSO for EAS analysis. Both IR and EAS the spectra of the recovered catalyst did not show any significant changes (**Supplementary Figures 17, 18**). This confirms that there was no leaching of OMs during the catalysis. The polymer network that is present in the hybrid prevents deterioration of OMs and provides the stability during oxidation of aniline.

## Electrochemical Measurements

The electrochemical properties of the hybrid materials were measured in 0.5 M  $H_2SO_4$  by cyclic voltammetry using the three electrode system. Cyclic voltammetry was carried out in a potential range between  $-0.2$  and 1 V at different scan rates ranging from 10 to 100 mV. **Figure 10A** represents the comparative CVs of different hybrid materials. The CV of the SOM-polymer hybrid shows the characteristic peaks of pure polyoxometalate. The cyclic voltammogram of the pure polymer does not show any noticeable activity. **Figure 10B** represents

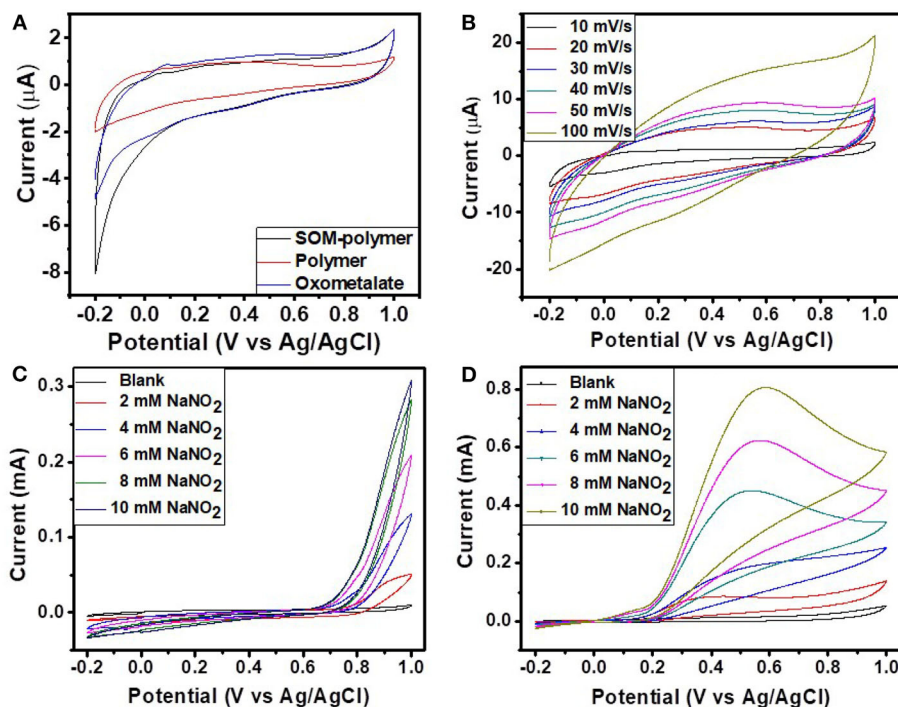


**FIGURE 10 |** (A) The comparison CVs of SOM-polymer, pure polymer, and pure oxometalate at a scan rate of 10 mV/s. (B) The CVs of the SOM-polymer hybrid at different scan rates ranging from 10 to 100 mV/s. CVs of (C) pure polymer and (D) SOM-polymer hybrid with different amounts of NaNO<sub>2</sub>. All of the electrochemical measurements were done in 0.5 M H<sub>2</sub>SO<sub>4</sub> using Ag/AgCl as a reference electrode.

the CVs of SOM-polymer hybrid at different scan rates (from 10 to 100 mV s<sup>-1</sup>). The cathodic and anodic peak current as well as peak separation potential gradually increase with increasing scan rate. The electrochemical stability of the OM-polymer hybrid was also measured. The OM-polymer hybrid electrode was studied under a continuous cycle with a scan rate of 50 mV s<sup>-1</sup> for 100 cycles. The cathodic and anodic peaks show very little change after the 100th cycle, which indicates very good stability of the hybrid. Compared to the hybrid, pure oxometalate is unstable and easily washed out during the electrochemical measurements.

We then explored whether it is possible to use this hybrid as a catalyst for an important oxidation reaction, the nitrite oxidation reaction. Nitrite is toxic to the human body. It forms nitrosamines and subsequently diazonium ions. The reactive diazonium ions disrupt normal cell function which leads to cell death. Nitrite can be detected by oxidation as well as reduction reaction. Though the reduction of nitrite is a little complicated, the oxidation reaction is pretty straight forward, which produces the only nitrate. Polyoxometalates are well-known for their catalytic activity. There are numerous reports of nitrite oxidation being performed by different catalytic materials but the question remains as to whether the SOM-polymer hybrid electrochemically catalyzes this reaction. In this article, we investigated nitrite oxidation using the SOM-polymer hybrid as a catalyst.

Nitrite oxidation of the SOM-polymer hybrid was performed in 0.5 M H<sub>2</sub>SO<sub>4</sub>, applying the potential range of -0.2 V to 1 V at a scan rate of 50 mV s<sup>-1</sup>. **Figure 10D** is a cyclic

voltammogram of nitrite oxidation reaction with SOM-polymer hybrid at different concentrations of nitrite ranging from 2 to 10 mM. The oxidation peak for the SOM-polymer hybrid was found at around 0.57 V with respect to the Ag/AgCl reference electrode, though peak shift was observed for different concentrations of NaNO<sub>2</sub>. The SOM-polymer hybrid showed an increase of 0.65 mA peak current for 10 mM NaNO<sub>2</sub> (**Figure 10D**). For a comparative study, we also performed the oxidation reaction with the pure polymer and pure polyoxometalate. There was no oxidation peak found in the same region for the polymer (**Figure 10C**) and negligible nitrite oxidation was observed for the pure polyoxometalate. The (C<sub>25</sub>H<sub>26</sub>N<sub>4</sub>)<sub>4</sub>[SiW<sub>11</sub>O<sub>39</sub>] also shows activity toward nitrite oxidation, though the current is not as high as in a polymer-SOM hybrid (**Supplementary Figures 1, 2**). This observation implies the emergence of catalytic activity of the SOM-Polymer hybrid that in a cascade catalyzes nitrite oxidation.

## CONCLUSIONS

To conclude, this study successfully grafted a polymerizable organic ion onto an oxometalate. The structure of the molecular hybrid was confirmed by the SCXRD pattern and the hybrid forms SOM in water DMSO mixture. The composite SOM, by the virtue of having a redox active oxometalate, polymerizes the side chain of tetrakis(4-aminophenyl)methane into a polymer. We characterized the polymeric structure by IR as well as



NMR spectra, thus creating a system for a polymer-colloid (SOM) mixture. This can be used for nitrite oxidation and the selective oxidation of aniline in a cascade catalytic mode. Thus in short we show first a self-assembly of an organic-inorganic hybrid SOM. By then exploiting the intrinsic redox property and acidity of the contained oxometalate in SOM, we oxidized the aniline based side chain to polyaniline. This polymer-SOM composite, in turn, owing to its intrinsic residual redox property, oxidizes aniline to nitrobenzene selectively, and electrochemically oxidizes nitrite to nitrate. We have thus shown, for the first time, cascade catalysis in the context of SOM chemistry, which could further explorations in the context of sustainable chemistry.

## DATA AVAILABILITY STATEMENT

The datasets generated for this study can be found in online repositories. The names of the repository/repositories and accession number(s) can be found at: CCDC, 1580136.

## REFERENCES

- Bar-Nahum, I., Cohen, H., and Neumann, R. (2003). Organometallic-polyoxometalate hybrid compounds: metallosalen compounds modified by Keggin type polyoxometalates. *Inorg. Chem.* 42, 3677–3684. doi: 10.1021/ic034095s
- Ben, T., Ren, H., Ma, S., Cao, D., Lan, J., Jing, X., et al. (2009). Targeted synthesis of a porous aromatic framework with high stability and exceptionally high surface area. *Angew. Chem.* 121, 9621–9624. doi: 10.1002/ange.200904637
- Chen, D., Sahasrabudhe, A., Wang, P., Dasgupta, A., Yuan, R., and Roy, S. (2013). Synthesis and properties of a novel quarternized imidazolium [ $\alpha$ -PW<sub>12</sub>O<sub>40</sub>]<sup>3-</sup> salt as a recoverable photo-polymerization catalyst. *Dalton Trans.* 42, 10587–10596. doi: 10.1039/c3dt32916j
- Cronin, L., and Müller, A. (2012). From serendipity to design of polyoxometalates at the nanoscale, aesthetic beauty and applications. *Chem. Soc. Rev.* 41, 7333–7334. doi: 10.1039/c2cs90087d
- Das, S., Lai, D., Mallick, A., and Roy, S. (2016a). Photo redox mediated inexpensive one-pot synthesis of 1, 4-diphenyl substituted butane-1, 4-dione from styrene using polyoxometalate as a catalyst. *ChemistrySelect* 1, 691–695. doi: 10.1002/slct.201500052
- Das, S., Misra, A., and Roy, S. (2016b). Enhancement of photochemical heterogeneous water oxidation by a manganese based soft oxometalate immobilized on a graphene oxide matrix. *New J. Chem.* 40, 994–1003. doi: 10.1039/C5NJ01099C
- Das, S., Misra, A., and Roy, S. (2016c). Light driven decarboxylative cross coupling of acrylic acid and iodobenzene using [Mo<sub>132</sub>] type keplerate as a catalyst. *Inorg. Chim. Acta.* 460, 77–82. doi: 10.1016/j.ica.2016.06.037
- Dolbecq, A., Dumas, E., Mayer, C. R., and Mialane, P. (2010). Hybrid organic-inorganic polyoxometalate compounds: from structural diversity to applications. *Chem. Rev.* 110, 6009–6048. doi: 10.1021/cr1000578
- Dong, Y., Das, S., Zhu, L., Ben, T., and Qiu, S. (2016). Standout electrochemical performance of SnO<sub>2</sub> and Sn/SnO<sub>2</sub> nanoparticles embedded in a KOH-activated carbonized porous aromatic framework (PAF-1) matrix as the anode for lithium-ion batteries. *J. Mater. Chem. A* 4, 18822–18831. doi: 10.1039/C6TA09384A
- Du, J., and Chen, Y. (2004). Preparation of organic/inorganic hybrid hollow particles based on gelation of polymer vesicles. *Macromolecules* 37, 5710–5716. doi: 10.1021/ma0497097
- Dualeh, A., Tétreault, N., Moehl, T., Gao, P., Nazeeruddin, M. K., and Grätzel, M. (2014). Effect of annealing temperature on film morphology of organic-inorganic hybrid perovskite solid-state solar cells. *Adv. Funct. Mater.* 24, 3250–3258. doi: 10.1002/adfm.201304022
- Fehse, K., Schwartz, G., Walzer, K., and Leo, K. (2007). Combination of a polyaniline anode and doped charge transport layers for high-efficiency organic light emitting diodes. *J. Appl. Phys.* 101:124509. doi: 10.1063/1.2748864
- Hagrman, P. J., Hagrman, D., and Zubieta, J. (1999). Organic-inorganic hybrid materials: from “simple” coordination polymers to organodiamine-templated molybdenum oxides. *Angew. Chem. Int. Ed.* 38, 2638–2684. doi: 10.1002/(SICI)1521-3773(19990917)38:18<2638::AID-ANIE2638>3.0.CO;2-4
- Heeger, A. J. (1993). Polyaniline with surfactant counterions: conducting polymer materials which are processible in the conducting form. *Synth. Met.* 57, 3471–3482. doi: 10.1016/0379-6779(93)90462-6
- Jeong, U., Im, S. H., Camargo, P. H., Kim, J. H., and Xia, Y. (2007). Microscale fish bowls: a new class of latex particles with hollow interiors and engineered porous structures in their surfaces. *Langmuir* 23, 10968–10975. doi: 10.1021/la702324q
- Kagan, C., Mitzi, D., and Dimitrakopoulos, C. (1999). Organic-inorganic hybrid materials as semiconducting channels in thin-film field-effect transistors. *Science* 286, 945–947. doi: 10.1126/science.286.5441.945
- Kikukawa, Y., Suzuki, K., Sugawa, M., Hirano, T., Kamata, K., Yamaguchi, K., et al. (2012). Cyanosilylation of carbonyl compounds with trimethylsilyl cyanide catalyzed by an yttrium-pillared silicotungstate dimer. *Angew. Chem.* 124, 3746–3750. doi: 10.1002/ange.201200486
- Kohut-Svelko, N., Pirri, R., Asua, J. M., and Leiza, J. R. (2009). Redox initiator systems for emulsion polymerization of acrylates. *J. Polym. Sci. A Polym. Chem.* 47, 2917–2927. doi: 10.1002/pola.23362
- Lachkar, D., Viloni, D., Dumont, E., Lelli, M., and Lacôte, E. (2016). Grafting of secondary diolamides onto [P<sub>2</sub>W<sub>15</sub>V<sub>3</sub>O<sub>62</sub>]<sup>9-</sup> generates hybrid heteropoly acids. *Angew. Chem. Int. Ed.* 55, 5961–5965. doi: 10.1002/anie.201510954
- Leng, W., Chen, M., Zhou, S., and Wu, L. (2010). Capillary force induced formation of monodisperse polystyrene/silica organic-inorganic hybrid hollow spheres. *Langmuir* 26, 14271–14275. doi: 10.1021/la102256t
- Liu, B., Ben, T., Xu, J., Deng, F., and Qiu, S. (2014). Hydrogen bonding controlled catalysis of a porous organic framework containing benzimidazole moieties. *New J. Chem.* 38, 2292–2299. doi: 10.1039/c4nj00053f
- Liu, S., Wang, J., Ou, J., Zhou, J., Chen, Y., and Yang, S. (2010). Fabrication of one dimensional polyaniline nanofibers by UV-assisted polymerization in the aqueous phase. *J. Nanosci. Nanotechnol.* 10, 933–940. doi: 10.1166/jnn.2010.1883
- Liu, T., Diemann, E., Li, H., Dress, A. W., and Müller, A. (2003). Self-assembly in aqueous solution of wheel-shaped Mo<sub>154</sub> oxide clusters into vesicles. *Nature* 426, 59–62. doi: 10.1038/nature02036

## AUTHOR CONTRIBUTIONS

KD, TY, and SP performed all the experiments and collected the data. SR conceived and designed the experiments and wrote the paper with input from all authors (particularly KD). Part of the experiments was performed in SR's laboratory and part in the facilities of TB and SQ. All authors read and approved the paper.

## ACKNOWLEDGMENTS

The authors thank the FIRE and PRIS grants of IISER-Kolkata and NSFC, China for financial support.

## SUPPLEMENTARY MATERIAL

The Supplementary Material for this article can be found online at: <https://www.frontiersin.org/articles/10.3389/fchem.2020.601814/full#supplementary-material>

- Liu, X., Kim, J.-S., Wu, J., and Eisenberg, A. (2005). Bowl-shaped aggregates from the self-assembly of an amphiphilic random copolymer of poly (styrene-co-methacrylic acid). *Macromolecules* 38, 6749–6751. doi: 10.1021/ma050665r
- Long, J. R., and Yaghi, O. M. (2009). The pervasive chemistry of metal–organic frameworks. *Chem. Soc. Rev.* 38, 1213–1214. doi: 10.1039/b903811f
- Lv, H., Geletii, Y. V., Zhao, C., Vickers, J. W., Zhu, G., Luo, Z., et al. (2012). Polyoxometalate water oxidation catalysts and the production of green fuel. *Chem. Soc. Rev.* 41, 7572–7589. doi: 10.1039/c2cs35292c
- Macdiarmid, A. G. (2001). “Synthetic metals:” a novel role for organic polymers (Nobel lecture). *Angew. Chem. Int. Ed.* 40, 2581–2590. doi: 10.1002/1521-3773(20010716)40:14<2581::AID-ANIE2581>3.0.CO;2-2
- Meenakshi, R., Shakeela, K., Kutti Rani, S., and Ranga Rao, G. J. C. L. (2018). Oxidation of aniline to nitrobenzene catalysed by 1-butyl-3-methylimidazolium phosphotungstate hybrid material using m-chloroperbenzoic acid as an oxidant. *Catal. Lett.* 148, 246–257. doi: 10.1007/s10562-017-2214-2
- Mostafaie, A., and Zolriasatein, A. (2012). Synthesis and characterization of conducting polyaniline nanocomposites containing ZnO nanorods. *Prog. Nat. Sci.: Mater. Int.* 22, 273–280. doi: 10.1016/j.pnsc.2012.07.002
- Paul, S., Sreejith, S., and Roy, S. (2018). pH-induced phase transition and crystallization of soft-oxometalates (SOMs) into polyoxometalates (POMs): a study on crystallization from colloids. *Acta Crystallogr. Sect. C Struct. Chem.* 74:1274. doi: 10.1107/S2053229618007143
- Pope, M., McCleverty, J. A., and Meyer, T. J. (2004). Comprehensive coordination chemistry II. *Transition Metal Groups* 3, 635–678. doi: 10.1016/B0-08-043748-6/03035-8
- Priewisch, B., and Rück-Braun, K. (2005). Efficient preparation of nitrosoarenes for the synthesis of azobenzenes. *J. Org. Chem.* 70, 2350–2352. doi: 10.1021/jo048544x
- Rana, U., Chakrabarti, K., and Malik, S. (2011). *In situ* preparation of fluorescent polyaniline nanotubes doped with perylene tetracarboxylic acids. *J. Mater. Chem.* 21, 11098–11100. doi: 10.1039/c1jm12051d
- Rausch, B., Symes, M. D., Chisholm, G., and Cronin, L. (2014). Decoupled catalytic hydrogen evolution from a molecular metal oxide redox mediator in water splitting. *Science* 345, 1326–1330. doi: 10.1126/science.1257443
- Ren, H., Ben, T., Wang, E., Jing, X., Xue, M., Liu, B., et al. (2010). Targeted synthesis of a 3D porous aromatic framework for selective sorption of benzene. *Chem. Commun.* 46, 291–293. doi: 10.1039/B914761F
- Rieger, J., Antoun, T., Lee, S. H., Chenal, M., Pembouong, G., Lesage De La Haye, J., et al. (2012). Synthesis and characterization of a thermoresponsive polyoxometalate–polymer hybrid. *Chem. Eur. J.* 18, 3355–3361. doi: 10.1002/chem.201101771
- Roy, S. (2011). “Soft oxometalates” (SOMs): a very short introduction. *Comments Inorg. Chem.* 32, 113–126. doi: 10.1080/02603594.2011.608443
- Roy, S. (2014). Soft-oxometalates beyond crystalline polyoxometalates: formation, structure and properties. *Crystengcomm* 16, 4667–4676. doi: 10.1039/C4CE00115J
- Sandre, O., Moreaux, L., and Brochard-Wyart, F. (1999). Dynamics of transient pores in stretched vesicles. *Proc. Natl. Acad. Sci. U. S. A.* 96, 10591–10596. doi: 10.1073/pnas.96.19.10591
- Sapurina, I., and Stejskal, J. (2008). The mechanism of the oxidative polymerization of aniline and the formation of supramolecular polyaniline structures. *Polym. Int.* 57, 1295–1325. doi: 10.1002/pi.2476
- Sapurina, I. Y., and Shishov, M. (2012). “Oxidative polymerization of aniline: molecular synthesis of polyaniline and the formation of supramolecular structures,” in *New Polymers for Special Applications*, ed A. D. S. Gomes (London, UK: IntechOpen), 272. doi: 10.5772/48758
- Shiraishi, Y., Sakamoto, H., Fujiwara, K., Ichikawa, S., and Hirai, T. (2014). Selective photocatalytic oxidation of aniline to nitrosobenzene by Pt nanoparticles supported on TiO<sub>2</sub> under visible light irradiation. *ACS Catal.* 4, 2418–2425. doi: 10.1021/cs500447n
- Shumaila, S., Lakshmi, G., Alam, M., Siddiqui, A. M., Zulfeqar, M., and Husain, M. (2011). Synthesis and characterization of Se doped polyaniline. *Curr. Appl. Phys.* 11, 217–222. doi: 10.1016/j.cap.2010.07.010
- Suzuki, K., Jeong, J., Yamaguchi, K., and Mizuno, N. (2015). Visible-light-responsive multielectron redox catalysis of lacunary polyoxometalates induced by substrate coordination to their Lacuna. *Chem. Asian J.* 10, 144–148. doi: 10.1002/asia.201403072
- Thomas, P., Chandel, S., Mallick, A., Sreejith, S., Ghosh, N., and Roy, S. (2018). Studying the crystallization of polyoxometalates from colloidal softoxometalates. *Cryst. Growth Des.* 18, 4068–4075. doi: 10.1021/acs.cgd.8b00443
- Thomas, P., Pei, C., Roy, B., Ghosh, S., Das, S., Banerjee, A., et al. (2015). Site specific supramolecular heterogeneous catalysis by optically patterned soft oxometalate–porous organic framework (SOM–POF) hybrid on a chip. *J. Mater. Chem. A* 3, 1431–1441. doi: 10.1039/C4TA01304B
- Tundo, P., Romanelli, G. P., Vázquez, P. G., Loris, A., and Aricò, F. (2008). Multiphase oxidation of aniline to nitrosobenzene with hydrogen peroxide catalyzed by heteropolyacids. *Synlett* 2008, 967–970. doi: 10.1055/s-2008-1072502
- Uribe-Romo, F. J., Hunt, J. R., Furukawa, H., Klöck, C., O’keeffe, M., and Yaghi, O. M. (2009). A crystalline imine-linked 3-D porous covalent organic framework. *J. Am. Chem. Soc.* 131, 4570–4571. doi: 10.1021/ja8096256
- Verhoeff, A. A., Kistler, M. L., Bhatt, A., Pigga, J., Groenewold, J., Klokkenburg, M., et al. (2007). Charge regulation as a stabilization mechanism for shell-like assemblies of polyoxometalates. *Phys. Rev. Lett.* 99:066104. doi: 10.1103/PhysRevLett.99.066104
- Verma, S., Hauck, T., El-Khouly, M. E., Padmawar, P. A., Canteenwala, T., Pritzker, K., et al. (2005). Self-assembled photoresponsive amphiphilic diphenylaminofluorene-C60 conjugate vesicles in aqueous solution. *Langmuir* 21, 3267–3272. doi: 10.1021/la047082f
- Wan, S., Guo, J., Kim, J., Ihee, H., and Jiang, D. (2009). A photoconductive covalent organic framework: self-condensed arene cubes composed of eclipsed 2D polypyrrene sheets for photocurrent generation. *Angew. Chem.* 121, 5547–5550. doi: 10.1002/ange.200900881
- Wang, S.-S., and Yang, G.-Y. (2015). Recent advances in polyoxometalate-catalyzed reactions. *Chem. Rev.* 115, 4893–4962. doi: 10.1021/cr500390v
- Wang, X., Liu, J., and Pope, M. (2003). New polyoxometalate/starch nanomaterial: synthesis, characterization and antitumoral activity. *Dalton Trans.* 5, 957–960. doi: 10.1039/b300920n
- Wang, Y., and Weinstock, I. A. (2012). Polyoxometalate-decorated nanoparticles. *Chem. Soc. Rev.* 41, 7479–7496. doi: 10.1039/c2cs35126a
- Xu, S., Roy, S., Ben, T., Pei, C., and Qiu, S. (2015). Enhanced recognition of a nitrogen containing organic compound by adjusting the acidity of the porous organic frameworks base (JUC-Z2). *J. Mater. Chem. A* 3, 2628–2633. doi: 10.1039/C4TA05640J
- Yasuda, A., and Shimidzu, T. (1993). Chemical oxidative polymerization of aniline with ferric chloride. *Polym. J.* 25:329. doi: 10.1295/polymj.25.329
- Yin, P., Bayaguud, A., Cheng, P., Haso, F., Hu, L., Wang, J., et al. (2014). Spontaneous stepwise self-assembly of a polyoxometalate–organic hybrid into catalytically active one-dimensional anisotropic structures. *Chem. Eur. J.* 20, 9589–9595. doi: 10.1002/chem.201402974
- Yin, P., Wang, J., Xiao, Z., Wu, P., Wei, Y., and Liu, T. (2012). Polyoxometalate–organic hybrid molecules as amphiphilic emulsion catalysts for deep desulfurization. *Chem. Eur. J.* 18, 9174–9178. doi: 10.1002/chem.201201551
- Zengin, H., Zhou, W., Jin, J., Czerw, R., Smith, D. W., Echegoyen, L., et al. (2002). Carbon nanotube doped polyaniline. *Adv. Mater.* 14, 1480–1483. doi: 10.1002/1521-4095(20021016)14:20<1480::AID-ADMA1480>3.0.CO;2-O
- Zhang, J., Song, Y. F., Cronin, L., and Liu, T. (2010). Reverse-vesicle formation of organic–inorganic polyoxometalate-containing hybrid surfactants with tunable sizes. *Chem. Eur. J.* 16, 11320–11324. doi: 10.1002/chem.201000794
- Zhu, Z., and Espenson, J. H. (1995). Kinetics and mechanism of oxidation of anilines by hydrogen peroxide as catalyzed by methylrhodium trioxide. *J. Org. Chem.* 60, 1326–1332. doi: 10.1021/jo00110a042

**Conflict of Interest:** The authors declare that the research was conducted in the absence of any commercial or financial relationships that could be construed as a potential conflict of interest.

Copyright © 2020 Das, Yan, Paul, Qiu, Ben and Roy. This is an open-access article distributed under the terms of the Creative Commons Attribution License (CC BY). The use, distribution or reproduction in other forums is permitted, provided the original author(s) and the copyright owner(s) are credited and that the original publication in this journal is cited, in accordance with accepted academic practice. No use, distribution or reproduction is permitted which does not comply with these terms.